# Mutation in Rod PDE6 Linked to Congenital Stationary Night Blindness Impairs the Enzyme Inhibition by Its $\gamma$-Subunit[†]

Khakim G. Muradov, Alexey E. Granovsky, and Nikolai O. Artemyev*,[‡]

*Department of Physiology and Biophysics, University of Iowa College of Medicine, Iowa City, Iowa 52242*

*Received October 31, 2002; Revised Manuscript Received January 9, 2003*

ABSTRACT: Photoreceptor cGMP phosphodiesterase (PDE6) is the effector enzyme in the vertebrate visual transduction cascade. The activity of rod PDE6 catalytic α- and $\beta$-subunits is blocked in the dark by two inhibitory P$\gamma$-subunits. The inhibition is released upon light-stimulation of photoreceptor cells. Mutation H258N in PDE6$\beta$ has been linked to congenital stationary night blindness (CSNB) in a large Danish family (Rambusch pedigree) (Gal, A., Orth, U., Baehr, W., Schwinger, E., and Rosenberg, T. (1994) *Nat. Genet*. *7*, 64−67.) We have analyzed the consequences of this mutation for PDE6 function using a P$\gamma$-sensitive PDE6α′/PDE5 chimera, Chi16. Biochemical analysis of the H257N mutant, an equivalent of PDE6$\beta$H258N, demonstrates that this substitution does not alter the ability of chimeric PDE to dimerize or the enzyme's catalytic properties. The sensitivity of H257N to a competitive inhibitor zaprinast was also unaffected. However, the mutant displayed a significant impairment in the inhibitory interaction with P$\gamma$, which was apparent from a ∼20-fold increase in the $K_i$ value (46 nM) and incomplete maximal inhibition. The inhibitory defect of H257N is not due to perturbation of noncatalytic cGMP binding to the PDE6α′ GAF domains. The noncatalytic cGMP-binding characteristics of the H257N mutant were similar to those of the parent PDE6α′/PDE5 chimera. Since rod PDE6 in the Rambusch CSNB is a catalytic heterodimer of the wild-type PDE6α and mutant PDE6$\beta$, Chi16 and H257N were coexpressed, and a heterodimeric PDE, Chi16/H257N, was isolated. It displayed two P$\gamma$ inhibitory sites with the $K_i$ values of 5 and 57 nM. Our results support the hypothesis that mutation H258N in PDE6$\beta$ causes CSNB through incomplete inhibition of PDE6 activity by P$\gamma$, which leads to desensitization of rod photoreceptors.

Photoreceptor cGMP phosphodiesterases (PDE6)[1] are activated in response to light stimulation of rod and cone cells. Activated PDE6 hydrolyzes intracellular cGMP resulting in a closure of cGMP-gated channels and hyperpolarization of the photoreceptor plasma membrane (*1*−*2*). Rod PDE6 is a catalytic heterodimer composed of the homologous PDE6 α and $\beta$ subunits associated with two copies of the inhibitory $\gamma$-subunit (P$\gamma$) (*3*−*6*). Mutations in the PDE6α and PDE6$\beta$ genes are responsible for 3−4% of cases of recessive retinitis pigmentosa (RP), a progressive retinal degeneration (*7*, *8*). These mutations are often nonsense or missense leading to substitutions of conserved residues within the noncatalytic cGMP-binding sites (GAF domains) or the catalytic domain. Missense mutations in PDE6α or PDE6$\beta$ in RP are likely to produce folding defects of the protein. The requirement of heterodimerization for expression of rod PDE6 leads to a complete loss of the functional enzyme in homozygotes despite only one of the genes being affected. The absence of PDE6 activity accompanied by elevation of cGMP levels had been described in animal models of retinal degeneration (*9*−*12*), and it might be responsible for recessive RP in humans. An increased intracellular cGMP level is thought to be a general cause of photoreceptor degeneration (*13*). A different type of mutation in the PDE6$\beta$ gene has been found in the Rambusch form of autosomal dominant congenital stationary night blindness (adCSNB) (*14*). The PDE6$\beta$H258N substitution appears to alter, rather than abolish, the rod PDE6 function. This mutation is not associated with retinal degeneration and results in nonprogressive night blindness because of loss of rod photoreceptor sensitivity. Such mutations are particularly interesting because a molecular mechanism of a disease-causing functional mutation can be examined experimentally. It has been hypothesized that the H258N mutation prevents full inactivation of rod PDE6, triggering CSNB in the Rambusch family (*14*). Constitutive activity of rod PDE6 leading to desensitization of dark-adapted photoreceptors would be consistent with the dominant nature of the disease. Experimental verification of this hypothesis or analysis of the consequences of the H258N mutation for PDE6 function has been lacking, owing to the absence of an expression system for PDE6 suitable for mutational analysis (*15*−*17*). To study the structure and function of PDE6, we have earlier developed a robust expression system of chimeras between cone PDE6α′ and cGMP-binding cGMP-specific PDE (PDE5 family) (*17*, *18*). In this study, we utilized Chi16, a PDE6α′/PDE5 chimera, to introduce the H257N substitution, a PDE6α′ equivalent of H258N (*18*). Chi16 contains 440

[†] This work was supported by National Institutes of Health Grant EY-10843.

* To whom correspondence should be addressed. Tel.: (319) 335-7864. Fax: (319) 335-7330. E-mail: nikolai-artemyev@uiowa.edu.

[‡] Established Investigator of the American Heart Association.

[1] Abbreviations: PDE, cGMP phosphodiesterase; PDE6, photoreceptor PDE; P$\gamma$, $\gamma$-subunit of PDE6; PDE5, cGMP-binding, cGMP-specific PDE (PDE5 family); adCSNB, autosomal dominant congenital stationary night blindness.

10.1021/bi027095x CCC: $25.00 
Published on Web 02/15/2003

N-terminal residues of PDE6α′ as well as the Pγ-binding site PDE6α′-737−784 within the catalytic domain. PDE6α′-737−784 confers upon Chi16 the sensitivity to Pγ (*18*). Therefore, Chi16 represented the best currently available template to address the mechanism of the Rambusch CSNB.

## EXPERIMENTAL PROCEDURES

*Materials*. cGMP was obtained from Boehringer Manheim. [$^3$H]cGMP was a product of Amersham Pharmacia Biotech. All restriction enzymes were purchased from NEB. AmpliTaq DNA polymerase was a product of Perkin-Elmer, and Pfu DNA polymerase was a product of Stratagene. Rabbit polyclonal anti-Pγ antibodies were from Affinity Bioreagents, Inc. Monoclonal anti-polyhistidine antibody, M2 monoclonal anti-flag antibody, zaprinast, and all other reagents were purchased from Sigma.

*Mutagenesis of Chi16.* DNA sequence coding for the residues 246−800 of Chi16 was PCR-amplified using the pFastBacHTbChi16 vector (*18*) as template. The 5′ PCR primer carried the SacI site (aa Glu248-Leu249) and the His257Asn substitution, and the 3′ PCR primer contained the XhoI site. The PCR product was ligated into pFastBacHTbChi16 using the SacI and XhoI sites. To construct flag-tagged Chi16, the flag-tag DNA sequence was first inserted into the pFastBacHTb vector replacing the His6 sequence. A DNA fragment was PCR-amplified using pFastBacHTb as a template, a 5′ primer containing an RsrII site and the flag tag sequence, and a 3′ primer containing a BamHI site. This DNA fragment was then ligated with the large RsrII/BamHI fragment of pFastBacHTb to produce pFastBacflag. DNA coding Chi16 was inserted into pFastBacflag using NarI and XhoI restriction sites. The sequences of the constructs were verified by automated DNA sequencing at the University of Iowa DNA Core Facility.

*Expression and Purification of Chi16 and the H257N Mutant.* Generation of the recombinant bacmids, transfection of Sf9 cells, and viral amplifications were carried out according to the manufacturer's recommendations (Life Technologies, Inc.). For Chi16 and H257N protein expression, Sf9 cell cultures ($2 \times 10^6$ cells/mL) were infected with baculoviruses at MOI of 3−10. Cells were harvested by centrifugation at 55 h after infection; washed with 20 mM Tris-HCl buffer (pH 8.0) containing 150 mM NaCl, 4 mM $MgSO_4$, and 5mM 2-mercaptoethanol; and processed immediately or stored at −80 °C until use. Sf9 cell pellets from 100 mL cell cultures were resuspended in 15 mL of 20 mM Tris-HCl buffer (pH 8.0) containing 2 mM $MgSO_4$, and one tablet of Complete Mini protease inhibitor cocktail (Roche Molecular Biochemicals). Cell lysates were obtained by sonication with four 20-s pulses using a flat tip attached to a 550 Sonic Dismembrator (Fisher Scientific) and cleared by centrifugation (100 000*g*, 90 min, 4 °C). Chi16 and H257N were partially purified using affinity chromatography on a His-bind resin (Novagen) as described earlier (*18*). To obtain heterodimeric PDE, Chi16/H257N, a flag-tagged Chi16 was coexpressed with a His-tagged H257N in Sf9 cells. Following purification of the cell extracts on a His-bind resin, Chi16/H257N was isolated using an anti-flag M2-agarose affinity gel (Sigma). The affinity chromatography was performed according to the manufacturer's recommendations using Flag peptide (Sigma) to elute Chi16/H257N. Purified proteins were dialyzed against 40% glycerol and stored at −20 °C.

*Analysis of Dimerization of Chi16 and H257N by Gel Filtration.* Chi16, H257N, and Chi16/H257N samples (100 μL) were injected into a Superose 12 10/30 column (Amersham Pharmacia Biotech) equilibrated with 30 mM Tris-HCl buffer (pH 8.0) containing 100 mM NaCl and 2 mM $MgSO_4$. Proteins were eluted at 0.4 mL/min, and 0.4 mL fractions were collected. Each fraction was assayed for PDE activity and the presence of Chi16 and H257N by Western blotting. Western blot analysis of the gel filtration fractions was performed following SDS−PAGE in 10% gels (*19*). Monoclonal anti-polyhistidine antibodies and M2 monoclonal anti-flag were used with dilutions 1:1500 and 1:5000, respectively. The antibody−antigen complexes were detected using anti-mouse antibodies conjugated to horseradish peroxidase (Sigma) and ECL reagent (Amersham Pharmacia Biotech.).

*Immunoprecipitation.* Pγ (15 nM) was mixed on ice with Chi16 or H257N (1 nM) in 200 μL of 10 mM Tris-HCl buffer (pH 7.4) containing 150 mM NaCl (TBS). Following incubation for 20 min, rabbit polyclonal anti-Pγ antibodies (2.5 μg) were added, and the mixture was incubated for another 60 min. Afterward, 10 μL of a 50% slurry of protein G-coupled agarose beads (Sigma) was added, and the mixture was incubated at +4 °C for 60 min. The agarose beads were washed with TBS (4 × 1 mL), and the bound proteins were eluted with an SDS−PAGE sample buffer for separation on 10% gels and Western blot analysis with monoclonal anti-polyhistidine antibodies.

*cGMP-Binding Assay.* The cGMP-binding assay was performed in a total volume of 100 μL of 10 mM HEPES-Na buffer (pH 7.0), containing 1.5 pmol of Chi16 or H257N, 1 mM EDTA, 10 mM 2-mercaptoethanol, 100 μM zaprinast, [H$^3$]cGMP (60 000 cpm), and varying concentrations of unlabeled cGMP. The binding reactions were incubated for 30 min at 4 °C and then applied onto wet 0.45 μm cellulose nitrate membrane filters (Whatman, England). The filters were washed three times with ice-cold PBS buffer containing 1 mM EDTA (6 mL total volume), dried, and counted in a liquid scintillation counter after dissolution in a counting cocktail. No cGMP hydrolysis was detected under the conditions of the cGMP-binding assay.

*Other Methods*. PDE activity was measured using [$^3$H]-cGMP as described (*20*, *21*). Less than 15% of cGMP was hydrolyzed during these reactions. The $K_i$ values for inhibition of PDE activity by Pγ and zaprinast were measured using 50 pM Chi16 (or H257N) and 0.5 μM cGMP (i.e., <35% of $K_m$ value for chimeric and mutant PDEs). The $K_i$ ($IC_{50}$) values were calculated by fitting the data to eqs 1 (Figures 2B and 3) and 2 (Figure 5B)

$$Y = B + \frac{T - B}{1 + 10^{(X - \log K_i)}} \quad (1)$$

$$Y = B + \frac{0.5(T - B)}{1 + 10^{(X - \log K_{i1})}} + \frac{0.5(T - B)}{1 + 10^{(X - \log K_{i2})}} \quad (2)$$

where B (bottom) is PDE activity at infinite concentration of Pγ (or zaprinast), T (top) is PDE activity in the absence of Pγ (or zaprinast), and $X$ is the logarithm of total Pγ (or zaprinast) concentration. Concentrations of Chi16, H257N,

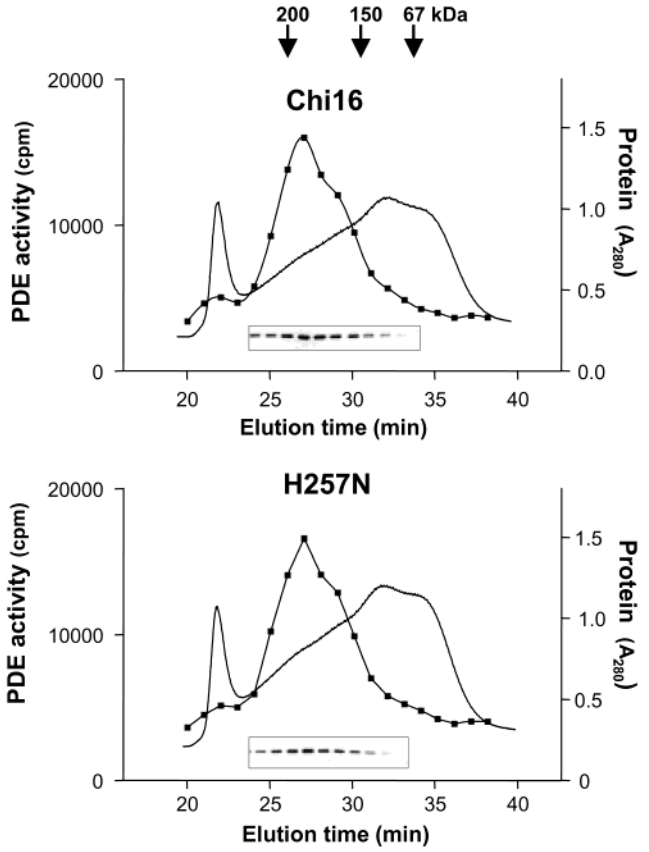


FIGURE 1: Dimerization of Chi16 and the H257N mutant. Chi16 and H257N were expressed individually in Sf9 cells. Chi16 and H257N partially purified on a His-bind resin were subjected to a FPLC gel filtration on a calibrated Superose 12 10/30 column (Amersham Pharmacia Biotech). Fractions of 0.4 mL were collected and analyzed for PDE activity (■) and by Western blotting with monoclonal anti-polyhistidine antibody (insets).

and a heterodimeric Chi16-H257N used in the inhibition experiments were much lower than the observed $K_i$ values, and the maximal corrections of the $K_i$ values using free P$\gamma$ concentrations would not exceed 3%. Protein concentrations were determined by the method of Bradford (*22*) using IgG as a standard. The molar concentrations of Chi16 and H257N were calculated based on the fraction of PDE protein in preparations, and the MW of 186.0 kDa for the catalytic dimers. The fractional concentrations of PDE were determined from analysis of the Coomassie Blue stained SDS gels using a HP ScanJet II CX/T scanner and Scion Image Beta 4.02 software. A typical fraction of Chi16 and H257N in partially purified preparations was 10−15%. The $k_{cat}$ values for cGMP hydrolysis were calculated as $V_{max}$/[PDE]. Fitting the experimental data to equations was performed with nonlinear least squares criteria using GraphPad Prizm Software. The $K_i$, $K_m$, and $IC_{50}$ values are expressed as mean ± SE for three independent measurements.

## RESULTS

*Dimerization and Catalytic Characteristics of the H257N Mutant.* Substitution PDE6α′H257N corresponding to the CSNB-related mutation of PDE6$\beta$, H258N, was introduced into the P$\gamma$-sensitive PDE6α′/PDE5 chimera, Chi16 (*18*). The mutant was expressed in Sf9 insect cells as His-tagged protein and purified using affinity chromatography on His-bind resin. The level of expression of H257N in Sf9 cells was 1.5−2-fold higher to that of Chi16 with a typical yield of the soluble protein of 100−150 $\mu$g/L of culture. We first assessed if the substitution of the His residue causes any detectable folding defect in mutant PDE. Folding deficiencies in PDE subunits are likely to interfere with correct dimerization of the enzyme, which would impact its stability and function. The ability of H257N to dimerize was examined using FPLC gel filtration on a Superose 12 HR 10/30 column calibrated using native PDE6, recombinant wild-type PDE5, and molecular weight standards. The profile of elution of mutant PDE as well as the profile of cGMP-hydrolytic activity in gel filtration fractions indicates that the mutation H257N does not affect the ability of Chi16 to form dimeric PDE species (Figure 1).

Next, the catalytic characteristics of H257N have been examined in comparison with Chi16. The $k_{cat}$ (9.4 mol mol $PDE^{-1}$ $s^{-1}$) and $K_m$ (4.3 $\mu$M) values for cGMP hydrolysis by H257N were comparable to those of Chi16 (Figure 2A).

Zaprinast, a specific competitive inhibitor of PDE5 and PDE6, has been utilized to further probe the properties of the catalytic pocket the Chi16 mutant. The $IC_{50}$ value for inhibition of H257N by zaprinast (0.24 $\mu$M) was similar to that of Chi16 (0.22 $\mu$M) (Figure 2B).

*Inhibition of the H257N Mutant by P$\gamma$.* The analysis of the inhibition of cGMP-hydrolytic activity of H257N by P$\gamma$ was carried out in relation to Chi16. The H257N substitution considerably reduced the ability of P$\gamma$ to inhibit the enzyme activity. The defects in the inhibitory interaction of H257N with P$\gamma$ were of two kinds. The $K_i$ value for H257N was ∼20-fold higher than that for Chi16, and the maximal inhibition was incomplete (Figure 3A). The fitting curves to a sigmoidal dose−response with Hill slope $H = 1$ (eq 1) for Chi16 ($R^2 = 0.985$) and for H257N ($R^2 = 0.98$) yielded PDE activities at infinite [P$\gamma$] of 15 and 26%, respectively. The effect of H257N mutation on the maximal inhibition is moderate and might be secondary to a more profound P$\gamma$-binding defect. Fitting the data to the equation with variable Hill slope produced $H = 0.9$ for Chi16 and $H = 0.95$ for H257N and did not meaningfully improve the goodness of fit ($R^2$ value) for both sets of data (not shown). This suggests a lack of cooperativity between the two equivalent P$\gamma$-binding sites in the catalytic dimers. The P$\gamma$-binding impairment of H257N inferred from the increase in the $K_i$ value was confirmed by immunoprecipitation of the P$\gamma$−Chi16 and P$\gamma$−H257N complexes using anti-P$\gamma$ antibodies. The reduction in immunoprecipitation of the P$\gamma$−H257N complex indicates a lower affinity of P$\gamma$ for the mutant PDE (Figure 3, inset).

*Noncatalytic cGMP Binding to H257N.* The residue His257 is localized within the N-terminal regulatory domain of PDE6α′, which is involved in noncatalytic cGMP binding to PDE6. Noncatalytic cGMP binding has been shown to modulate the affinity of interaction of PDE6 catalytic subunits with P$\gamma$ (*23*, *24*). The binding of cGMP to the noncatalytic sites of H257N was investigated to test the possibility that impairment in noncatalytic cGMP binding may have caused deficient inhibition of H257N by P$\gamma$. The binding experiments, however, demonstrated that the affinity ($K_d = 44$ nM) and stoichiometry (0.43 mol cGMP/mol PDE subunit) of binding of cGMP to noncatalytic sites were essentially unchanged in the mutant PDE as opposed to Chi16 ($K_d = 55$ nM, 0.40 mol/mol) (Figure 4).

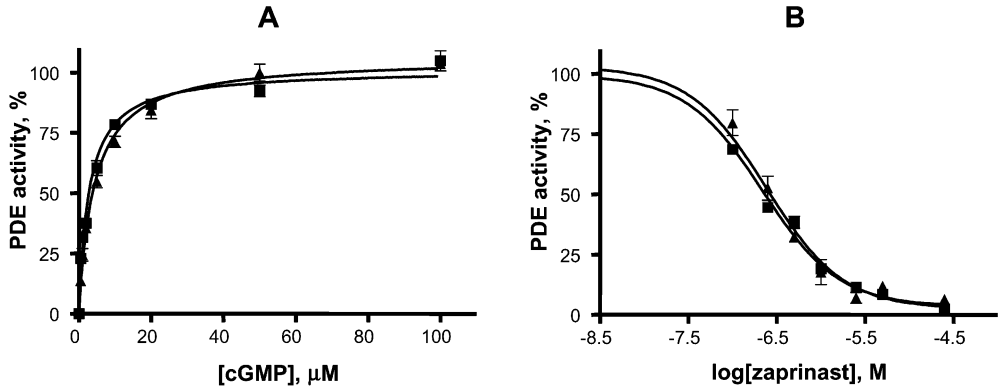


FIGURE 2: Catalytic properties of Chi16 and the H257N mutant. (A) PDE activities of Chi16 (■) and H257N (▲) were determined using 0.1 $\mu$Ci of [$^3$H]cGMP and increasing concentrations of unlabeled cGMP. The rates of cGMP hydrolysis are expressed as a percentage of maximal activity of Chi16 (9.0 mol of cGMP mol PDE$^{-1}$ s$^{-1}$). H257N hydrolyzed cGMP with the maximal activity of 9.4 mol of cGMP mol PDE$^{-1}$ s$^{-1}$. The $K_m$ values of 2.8 ± 0.3 $\mu$M for Chi16 and 4.3 ± 0.3 $\mu$M for H257N are calculated from the fitting curves. (B) Inhibition of PDE activities of Chi16 (■) and H257N (▲) by zaprinast. The rates of cGMP hydrolysis of Chi16 and H257N (50 pM) were determined in the presence of 0.5 $\mu$M cGMP, and increasing concentrations of zaprinast and are expressed as a percentage of the respective PDE activity in the absence of zaprinast. The calculated $IC_{50}$ values for Chi16 and H257N are 0.22 ± 0.01 and 0.24 ± 0.02 $\mu$M, respectively.

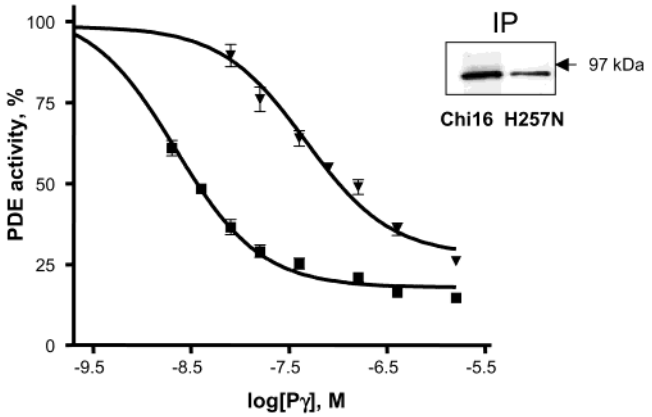


FIGURE 3: Interaction of P$\gamma$ with Chi16 and H257N. The activities of Chi16 (■) and H257N (▼) (50 pM) were determined in the presence of 0.5 $\mu$M cGMP and increasing concentrations of P$\gamma$ and are expressed as a percentage of the respective PDE activity in the absence of P$\gamma$. The P$\gamma$-inhibition data were fit to eq 1. The calculated $K_i$ values for Chi16 and H257N are 2.2 ± 0.1 and 46 ± 7 nM, respectively. IP: The P$\gamma$−Chi16 and P$\gamma$−H257N complexes were formed, immunoprecipitated using anti-P$\gamma$ antibodies and protein G-agarose beads, and analyzed by Western blotting with anti-polyhistidine antibodies as described under Experimental Procedures.

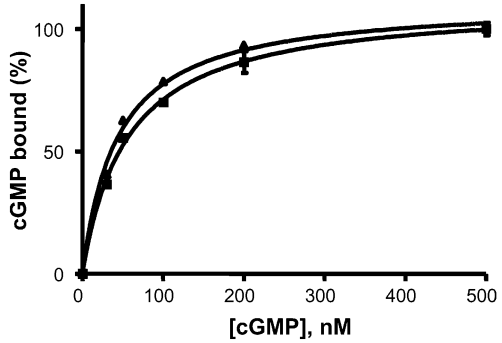


FIGURE 4: Noncatalytic cGMP binding to Chi16 and H257N. Binding of cGMP to Chi16 (■) and H257N (▲) was carried out for 30 min at 4 °C using [H$^3$]cGMP (60 000 cpm) and varying concentrations of unlabeled cGMP. The bound cGMP was determined by the filter-binding assay and is expressed as a percentage of maximal noncatalytic cGMP binding to Chi16 (0.4 mol cGMP/mol PDE subunit). The calculated $K_d$ values for Chi16 and H257N are 55 ± 4 and 44 ± 3 nM, respectively.

*Inhibition of Chi16/H257N Heterodimer by P$\gamma$.* In the Rambusch form of adCSNB, the PDE6$\beta$258N mutant subunit forms a heterodimer with the normal PDE6α subunit. Therefore, a heterodimer between Chi16 and H257N represents a more appropriate model than a homodimer of H257N to address the biochemical mechanism of the disease. To investigate dimerization between Chi16 and H257N and the P$\gamma$ inhibition of the heterodimer, a flag-tagged Chi16 was coexpressed with a His-tagged H257N in Sf9 cells. Heterodimeric PDE, Chi16/H257N, was purified from Sf9 cell lysates by sequential affinity chromatography on His-bind resin and anti-flag antibody-coupled agarose and analyzed by gel filtration on a Superose 12 HR 10/30 column (Figure 5A). A PDE activity peak corresponding to the dimeric PDE species contained both anti-His and anti-flag signals confirming formation of a heterodimer between Chi16 and H257N (not shown). Analysis of inhibition of Chi16/H257N revealed that the P$\gamma$-inhibitory defect is retained in the heterodimer. Fitting the Chi16/H257N inhibition data to eq 1 produced an apparent $K_i$ value of 16 nM (not shown), but the quality of fit was relatively poor ($R^2 = 0.96$). A significantly better fit ($R^2 = 0.975$) was obtained when eq 2 for a two-site inhibition with equal concentrations (fractions) of inhibitory sites was used (Figure 5B). The $K_i$ values of 5.0 and 57 nM were calculated from the inhibition curve.

## DISCUSSION

Three major components (rhodopsin, transducin, and PDE6) transduce and amplify the signal in the vertebrate visual transduction cascade. Mutations in the three genes coding the key photoexcitation proteins, rhodopsin, the rod transducin α-subunit (Gtα), and the rod PDE6 $\beta$-subunit have been linked to stationary night blindness (*25*). Major attributes of the adCSNB caused by defects in these genes are similar. They include a severe reduction in rod sensitivity (∼100−1000-fold), which does not recover under dark-adapted conditions. The cone function remains normal or modestly impaired (*25*). This results in nearly normal cone-mediated daytime vision but poor rod-mediated nighttime vision. The molecular mechanism for CSNB caused by mutations in the rhodopsin gene had been revealed when in vitro studies demonstrated constitutive activity of the opsin

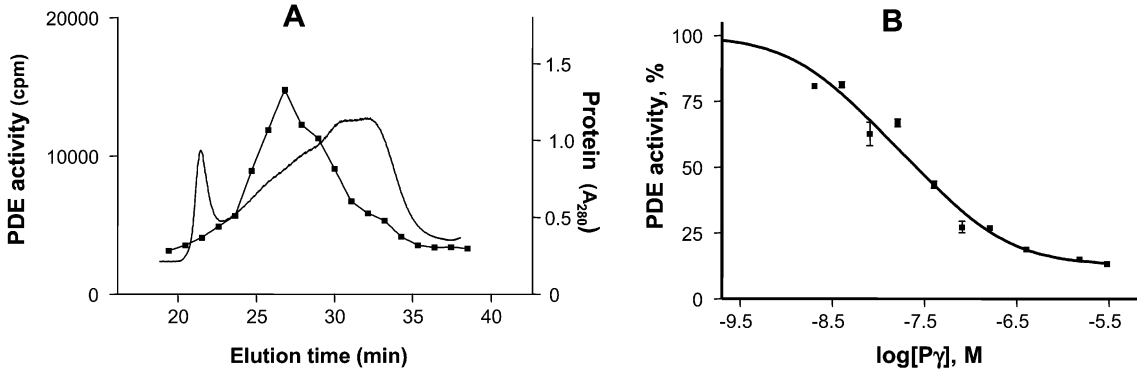


FIGURE 5: Dimerization of Chi16 with H257N and effect of P$\gamma$ on the heterodimeric PDE. (A) Chi16 and H257N were coexpressed in Sf9 cells. Heterodimeric PDE, Chi16/H257N, was purified from Sf9 cell lysates by sequential affinity chromatography on His-bind resin and anti-flag antibody-coupled agarose and analyzed by FPLC gel filtration on a calibrated Superose 12 10/30 column (Amersham Pharmacia Biotech). Fractions of 0.4 mL were collected and analyzed for PDE activity (■). (B) The activity of Chi16/H257N (50 pM) was determined in the presence of 0.5 $\mu$M cGMP and increasing concentrations of P$\gamma$ and is expressed as a percentage of the PDE activity in the absence of P$\gamma$. The P$\gamma$-inhibition data were fit to eq 2. $K_{i1}$ of 5.0 ± 1.1 nM and $K_{i2}$ of 57 ± 15 nM are calculated from the fitting curve.

mutants, A292E and G90D (*26*, *27*). The continuous activation of the visual cascade by the mutant opsins apparently produces desensitization of rod photoreceptors. The clinical parallels between the forms of CSNB related to rhodopsin, Gtα, and PDE6$\beta$ indicate that constitutive activation of the cascade might be a common mechanism for the visual disorders. Continuous activity of PDE6 has been hypothesized as a molecular mechanism for the Rambusch form of CSNB, when a perfect co-segregation of the PDE6$\beta$H258N mutation with the disease phenotype had been discovered (*14*). Likewise, a constitutive activation of transducin has been proposed as a leading cause for the Nougaret form of CSNB linked to the G38D mutation in Gtα (*28*). Bolstering this hypothesis, Gly38 of transducin is a counterpart of Gly12 in p21ras. Mutations of Gly12 render p21ras oncogenic because of its constitutive activity caused by the defect in GTPase activity (*29*−*31*). However, our previous biochemical analysis of GtαG38D in vitro has produced an unexpected result—GtαG38D fails to interact with and activate PDE6 (*32*). Therefore, in contrast to constitutive activation of the visual cascade in the rhodopsin-related forms of CSNB, the Nougaret form may have its molecular origin in the loss of the transducin effector function. It should be noted that this mechanism does not provide an obvious explanation for the dominant phenotype of the G38D mutation. GtαG38D may act as a dominant-negative mutant in the visual tansduction cascade, but experimental evidence supporting this notion has not yet been developed. To investigate the mechanism of the Rambusch form of CSNB, we generated the PDE6α′ H257N mutant using a P$\gamma$-sensitive PDE6α′/PDE5 chimera, Chi16 (*18*). The biochemical analysis of this mutant PDE revealed generally intact dimerization, noncatalytic cGMP binding, and catalytic properties of the enzyme. The only clearly affected function of H257N was its impaired interaction with P$\gamma$. The inhibitory defect of H257N manifested itself in a significant ∼20-fold increase in the $K_i$ value coupled with the incomplete PDE activity block at high concentrations of P$\gamma$. Rod PDE6 in the Rambusch CSNB is a catalytic heterodimer of the wild-type PDE6α and mutant PDE6$\beta$. Our model of the mutant heterodimeric PDE6, Chi16/H257N, exhibited a two-site inhibitory interaction with P$\gamma$. One of the sites had a significantly lower affinity for P$\gamma$, likely reflecting the presence of the mutant subunit. This finding suggests that, as it was hypothesized earlier (*14*), an incomplete inactivation of PDE6 by P$\gamma$ in the dark leading to desensitization of rod photoreceptors is responsible for the disease phenotype. The structural basis for the defective interaction of H257N (PDE6$\beta$H258N) with P$\gamma$ is not clear. According to the primary structure, PDE6 catalytic subunits contain two N-terminally located GAF regions (GAFa: ∼PDE6$\beta$-52−218 and GAFb: ∼PDE6$\beta$-253−441) and the C-terminal catalytic region (*6*, *33*, *34*). These regions also appear as three distinct three-dimensional domains in images of rod PDE6 obtained by electron microscopy (*35*). The His residue is located within the GAFb domain. P$\gamma$ has been shown to interact with the GAFa and catalytic domains of PDE6 (*36*−*38*). Using synthetic peptides, a potential P$\gamma$-interaction site was found in PDE6$\beta$ residues 211−230 (*39*), corresponding to a region linking the GAF domains. However, a direct interaction of P$\gamma$ with the GAFb domain has not been demonstrated. It appears likely that the effect of the His substitution is indirect. A positive cooperativity between the P$\gamma$ and the noncatalytic cGMP-binding sites in PDE6 (*23*, *24*, *40*, *41*) suggests that the inhibitory defect in the mutant PDE6 could have been mediated by perturbation of cGMP binding to the enzyme GAF domains. But the intact cGMP-binding characteristics of H257N do not support the involvement of noncatalytic cGMP. An alternative mechanism for the indirect effect is a mutation-induced conformational change in PDE6 leading to the reduced affinity for P$\gamma$. A potential for significant structural flexibility of GAF-containing PDEs has been highlighted by demonstration of ligand-induced conformational changes in PDE5 (*42*). In the presence of cGMP and a broad PDE inhibitor, 3-isobutyl-1-methylxantine, PDE5 assumed a less compact conformation as determined by gel filtration and native gel electrophoresis (*42*). Using similar approaches, gel filtration (Figure 1) and native gel electrophoresis (not shown), we have not detected notable conformational differences between Chi16 and H257N in the absence or presence of cGMP, zaprinast, and/or P$\gamma$. However, the yield of H257N expression in Sf9 cells was consistently higher than that of Chi16. Furthermore, a sample of H257N always produced a stronger Western blot signal following an overnight electrophoresis run in a native gel than an equivalent sample of Chi16 (not shown). These are likely indications of increased solubility (hydrophilicity) of H257N in comparison to Chi16, which may reflect conformational differences between the proteins.

## REFERENCES


1. Chabre, M., and Deterre, P. (1989) *Eur. J. Biochem. 179*, 255−266.
2. Yarfitz, S., and Hurley, J. B. (1994) *J. Biol. Chem. 269*, 14329−14332.
3. Baehr, W., Devlin, M. J., and Applebury, M. L. (1979) *J. Biol. Chem. 254*, 11669−11677.
4. Hurley, J. B., and Stryer, L. (1982) *J. Biol. Chem. 257*, 11094−11099.
5. Deterre, P., Bigay, J., Forquet, F., Robert, M., and Chabre, M. (1988) *Proc. Natl. Acad. Sci. U.S.A. 85*, 2424−2428.
6. Lipkin, V. M., Khramtsov, N. V., Vasilevskaya, I. A., Atabekova, N. V., Muradov, K. G., Li, T., Johnston, J. P., Volpp, K. J., and Applebury, M. L. (1990) *J. Biol. Chem. 265*, 12955−12959.
7. Dryja, T. P., Rucinski, D. E., Chen, S. H., and Berson, E. L. (1999) *Invest. Ophthalmol. Vis. Sci. 40*, 1859−1865.
8. McLaughlin, M. E., Ehrhart, T. L., Berson, E. L., and Dryja T. P. (1995) *Proc. Natl. Acad. Sci. U.S.A. 92*, 3249−3253.
9. Farber, D. B., and Lolley, R. N. (1974) *Science 186*, 449−451.
10. Farber, D. B., and Lolley, R. N. (1976) *J. Cyclic Nucleotide Res. 2*, 139−148.
11. Aquirre, G., Farber, D., Lolley, R., Fletcher, R. T., and Chader, G. J. (1978) *Science 201*, 1133−1134.
12. Suber, M. L., Pittler, S. J., Qin, N., Wright, G. C., Holcombe, V., Lee, R. H., Craft, C. M., Lolley, R. N., Baehr, W., and Hurwitz, R. L. (1993) *Proc. Natl. Acad. Sci. U.S.A. 90*, 3968−3972.
13. Lolley, R. N., Farber, D. B., Rayborn, M. E., and Hollyfield, J. G. (1977) *Science 196*, 664−666.
14. Gal, A., Orth, U., Baehr, W., Schwinger, E., and Rosenberg, T. (1994) *Nat. Genet. 7*, 64−67.
15. Piriev, N. I., Yamashita, C., Samuel, G., and Farber, D. (1993) *Proc. Natl. Acad. Sci. U.S.A. 90*, 9340−9344.
16. Qin, N., and Baehr, W. (1994) *J. Biol. Chem. 269*, 3265−3271.
17. Granovsky, A. E., Natochin, M., McEntaffer, R. L., Haik, T. L., Francis, S. H., Corbin, J. D., and Artemyev, N. O. (1998) *J. Biol. Chem. 273*, 24485−24490.
18. Granovsky, A. E., and Artemyev, N. O. (2000) *J. Biol. Chem. 275*, 41258−41262.
19. Laemmli, U. K. (1970) *Nature 227*, 680−685.
20. Thompson, W. J., and Appleman, M. M. (1971) *Biochemistry 10*, 311−316.
21. Natochin, M., and Artemyev, N. O. (2000) *Methods Enzymol. 315*, 539−554.
22. Bradford, M. M. (1976) *Anal. Biochem. 72*, 248−254.
23. Arshavsky, V. Y., Dumke, C. L., and Bownds, M. D.(1992) *J. Biol. Chem. 267*, 24501−24507.
24. Mou, H., and Cote, R. H. (2001) *J. Biol. Chem. 276*, 27527−27534.
25. Dryja, T. P. (2000) *Am. J. Ophthalmol. 130*, 547−563.
26. Dryja, T. P., Berson, E. L., Rao, V. R., and Oprian, D. D. (1993) *Nat. Genet. 4*, 280−283.
27. Rao, V. R., Cohen, G. B., and Oprian, D. D. (1994) *Nature 367*, 639−642.
28. Dryja, T. P., Hahn, L. B., Reboul, T., and Arnaud, B. (1996) *Nat. Genet. 13*, 358−360.
29. Barbacid, M. (1987) *Annu. Rev. Biochem. 56*, 779−828.
30. Seeburg, P. H., Colby, W. W., Capon, D. J., Goeddel, D. V., and Levinson, A. D. (1984) *Nature 312*, 71−75.
31. Trahey, M., and McCormick, F. (1987) *Science 238*, 542−545.
32. Muradov, K. G., and Artemyev N. O. (2000) *J. Biol. Chem. 275*, 6969−6974.
33. Aravind, L., and Ponting, C. P. (1997) *Trends Biochem. Sci. 22*, 458−459.
34. Martinez, S. E., Wu, A. Y., Glavas, N. A., Tang, X. B., Turley, S., Hol, W. G., and Beavo, J. A. (2002) *Proc. Natl. Acad. Sci. U.S.A. 99*, 13260−13265.
35. Kameni Tcheudji, J. F., Lebeau, L., Virmaux, N., Maftei, C. G., Cote, R. H., Lugnier, C., and Schultz, P. (2001) *J. Mol Biol. 310*, 781−791.
36. Artemyev, N. O., Natochin, M., Busman, M., Schey, K. L., and Hamm, H. E. (1996) *Proc. Natl. Acad. Sci. U.S.A. 93*, 5407−5412.
37. Granovsky A. E., Natochin M., and Artemyev, N. O. (1997) *J. Biol. Chem. 272*, 11686−11669.
38. Muradov, K. G., Granovsky, A. E., Schey, K. L., and Artemyev, N. O. (2002) *Biochemistry 41*, 3884−3890.
39. Oppert, B., and Takemoto, D. J. (1991) *Biochem. Biophys. Res. Commun. 178*, 474−479.
40. Yamazaki, A., Bartucca, F., Ting, A., and Bitensky, M. W. (1982) *Proc. Natl. Acad. Sci. U.S.A. 79*, 3702−3706.
41. Cote, R. H., Bownds, M. D., and Arshavsky, V. Y. (1994) *Proc. Natl. Acad. Sci. U.S.A. 91*, 4845−4849.
42. Francis, S. H., Chu, D. M., Thomas, M. K., Beasley, A., Grimes, K., Busch, J. L., Turko, I. V., Haik, T. L., and Corbin J. D. (1998) *Methods 14*, 81−92.


BI027095X